NJC

Accepted Manuscript

Journal Name

ARTICLE

Preparation of Dihydroquinazoline Carbohydrazone Fe(II) Complexes for Spin Crossover

Fu-Xing Shen,[a] Wei Huang,*[a] Takashi Yamamoto,[b] Yasuaki Einaga,[b] Dayu Wu[a]*

The dihydroquinazoline Fe[II] complexes, namely, [Fe(**pq-R**)$_2$](X)$_2$·xCH$_3$OH·yCH$_3$CN·zH$_2$O(R = 2-py: X = ClO$_4^-$, x = 1, y = 0, z = 2 (**1**), BF$_4^-$, x = 0, y = 2, z = 1.75 (**2**), CF$_3$SO$_3^-$, x = 1, y = 1, z = 0(**3**); and X = ClO$_4^-$: R = 2-OCH$_3$, x = 0, y = 0, z = 1(**4**), R = 3-OCH$_3$, x = 0, y = 0, z = 1(**5**)) were prepared and the effects of the solvent, counteranion and ligand substituent on spin crossover property were discussed. Comparison of X-ray diffraction data for these complexes revealed the sole presence of high-spin Fe[II] at 298 K and the bond distances around Fe[II] center at low temperature fall much closer to those at high temperature, which is consistent with variable-temperature dc magnetic susceptibility data. However, the loss of solvent induced the significant change of spin state for complex **1** and **2**. Moreover, fits to magnetic data of the desolvated samples provide crossover temperatures of $T_{1/2}$ = 182.9(6), 157.0(8) and 138.3(5) K for **1-des** (ClO$_4^-$), **2-des** (BF$_4^-$) and **3-des**(CF$_3$SO$_3^-$), respectively, indicative of the anion-dependent transition temperature. The cooperativity operating in the complexes is thought to be mainly from the intermolecular $\pi…\pi$ interactions between dihydroquinazoline rings on the neighboring molecules. The ligand substituent effect was also investigated on Fe[II] SCO property. This work revealed the spin crossover property of a new type of dihydroquinazoline Fe(II) complexes, including the transition temperature, the degree of completion and the cooperative nature of the transition, can be optimally designed when developing new spin-crossover materials.

Introduction

Spin-crossover (SCO) systems represent an exciting so-called bottom-up approach toward highly efficient and specific functional materials based on the idea that the miniaturisation limit of an electronic function reaches the molecule level and a molecule could work as electronic switches or memory storage devices.[1-3] These materials could undergo spin transition from a low spin (LS) to high spin (HS) state for d[4-7] electron configuration, i.e. especially Fe[II], through an external stimulus, such as thermal, pressure, light and etc.[4,5] The narrow range of ligand field strength for which a spin transition can occur makes these systems sensitive to the overall crystal lattice.[6-10] Hence, the pursuit of the novel ligand field that can implement the spin transition is crucial to fabricate this system. In addition, spin transition (ST) can occur either over a wide temperature range (gradual) or within a few degrees (abrupt) dependent on the high cooperativity between spin centers,

and so it can also produce thermal hysteresis.[11-15] Entities such as counterions,[16-18] ligand substituents[19-21] or lattice-solvent molecules[22-27] may have a drastic effect on the cooperativity of spin-transition properties of the material from gradual to steep temperature-dependent magnetic response.[28]

However, the exchange of counteranions frequently results in an annihilation of the SCO properties because the subtle structural variations are able to modify the ligand-field strength.[29-32] It's believed that the carbohydrazone derivative bearing N$_2$O binding site for metal center is an important scaffold for controlling SCO ligand field. However, up to now, whatever the carbohydrazone-containing or hydrazone-type ligands have been extremely rarely realized in the realm of iron spin crossover. The structurally characterised hydrazono-based iron(III) spin-crossover complex {[Fe(mph)$_2$](ClO$_4$)·0.5MeOH·0.5H$_2$O}$_2$ [Hmph = 2-methoxy-6-(pyridyl-2-ylhydrazonomethyl) phenol] possesses phenolate and pyridyl moieties.[33] Later on, Gao and coworkers reported the systematic modification of carbohydrazone-type Schiff base ligand for preparation of iron(II) complex, whose SCO property can be influenced by the ligand modification,[34] desolvation[35] and the particle size.[36] (Scheme 1) Another structurally characterized Fe(III) complex of this type is reported by Shongwe et al, who modified the ligand structure by substituting 4-hydoxy moiety with 4-*tert*-butyl change, as well as changing CH=N imine bond to C(Me)=N.[37] Despite the

SCO iron(II) complexes derived from carbohydrazone donors have been investigated in several cases, the predictability over the correlation between SCO property and the structure characteristic of the ligand is still desirable.

It should be noted that in the reported complexes mentioned above the carbohydrazone ligand is prone to be deprotonated upon metal coordination. Herein, the dihydroquinazoline derivatives were restrained by tunable 2-substituent groups were synthesized, which is expected to exhibit an appropriate ligand field and makes good candidates for the discovery of new SCO systems.[38,39] The synthesis, characterization and magnetic properties of a new series of compounds containing the cation [Fe(**pq-R**)$_2$]$^{2+}$ (**pq-R** = ((R-2-yl)methyleneamino)-2,3-dihydra-2-(pyridin-2-yl)quinazolin-4(1H)-one) with various anions, that is, ClO_4^- (**1**), BF_4^- (**2**) and $CF_3SO_3^-$(**3**) when fixing substituent of 2-pyridyl group and with modified substituents R = 2-methoxyl (**4**), and 3-methoxyl (**5**) when fixing anion of perchlorate, respectively, are fabricated to discuss the spin crossover property, while it allows detailed discussion of the collective influence of the solvent, counterion and ligand substituent on the structural and spin transition properties.
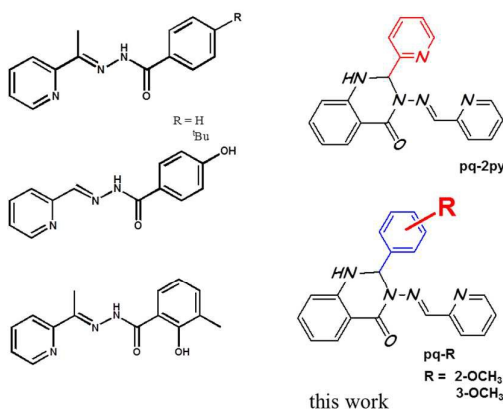
Scheme 1. Modified carbohydrazone series ligand for the formation of spin crossover Fe(II) complex in the related work.[34-37]

Experimental

General procedures and materials

All chemicals were purchased from Aldrich Co. Ltd and were used without further purification. All solvents were dried using standard procedures. Perdeuterated dimethyl sulfoxide (DMSO-d_6) was purchased from Alfa Aesar Co. Ltd and stored over 4 Å molecular sieves prior to use. Fe(CF$_3$SO$_3$)$_2$·2CH$_3$CN was synthesized according to a literature procedure.[40] Elemental analyses (C, H, and N) were conducted with a Perkin-Elmer 2400 analyzer. (**Caution!** Perchlorate salts are potentially explosive subject to heating, only complex **2** and **3** were used for TGA analysis). Micro-IR spectroscopy studies were performed on a Nicolet Magna-IR 750 spectrophotometer in the 4000-400 cm^{-1} region (w, weak; b, broad; m, medium; s, strong). Thermogravimetric analyses were conducted on NETZSCH TG 209 F3.^{1}H NMR spectra

were obtained from a solution in DMSO-d_6 using a Bruker-400 spectrometer. (s, singlet; d, doublet; t, triplet; m, multiplet; dd, double doublet). For the ^{57}Fe Mössbauer spectroscopic measurement, ^{57}Co in Rh was used as a Mössbauer source. The spectra were calibrated by using the six lines of a body-centered cubic iron foil (α-Fe), the center of which was taken as zero isomer shift. The experimental data of Mössbauer spectra were obtained in the cooling mode and fitted with a MossWinn 4.0 program.[41]

Magnetic Measurements

Magnetic susceptibility measurements were performed using a Quantum Design MPMS XL-7 SQUID magnetometer. The magnetic susceptibility measurements were taken while lowering the temperature from 300 to 5 K at the sweeping rate of 1 K min^{-1} under an applied magnetic field of 2500 Oe. Direct-current (dc) susceptibility measurements were taken on a freshly filtered crystal sample wrapped in a polyethylene membrane. Samples were prepared rapidly to avoid any loss of solvent for magnetic measurements. Corrections for diamagnetism were applied using Pascal's constants.[42]

Synthetic Procedure

2-aminobenzhydrazide and 2-amino-N'-(pyridin-2-ylmethylene)benzohydrazide were synthesized according to the literature method.[43]

Preparation of ligand 2-(pyridin-2-yl)-3-((pyridin-2-ylmethylene)amino)-2,3-dihydraquinazolin-4(1H)-one, [pq-2py]: This compound was synthesized through a modified literature procedure.[44] A mixture ethanolic solution of pyridine-2-carboxaldehyde (10.0 mmol, 1.0712 g) and 2-aminobenzhydrazide (5.0 mmol, 0.7559 g) was refluxed for 4 hours at the boiling temperature, after which a yellow microcrystalline solid was obtained. The product was washed with cold ethanol and dried in vacuo. Yield: 87%. ^{1}H NMR (400MHz, DMSO-d$_6$) δ 8.68 (s, 1H), 8.59(d, J=4.85, 1H), 8.48(d, J=4.18, 1H), 7.96(d, J=3.28, 1H),7.91(d, J=7.89, 1H),7.86(dd, 1H), 7.81(m, 1H), 7.73(d, J=6.78, 1H), 7.45(d, J=7.92, 1H), 7.40(m, 1H), 7.31(dd, 1H), 7.26(m, 1H), 6.78(d, J=8.07, 1H), 6.73(t, 1H), 6.65(d, J=3.49, 1H)ppm.

Preparation of ligand 2-(2-methoxyphenyl)-3-((pyridin-2-ylmethylene)amino)-2,3-dihydraquinazolin-4(1H)-one, [pq-2OCH$_3$]: 2-Methoxybenzaldehyde (5 mmol, 0.6808 g) was added to a solution of 2-amino-N'-(pyridin-2-ylmethylene)benzohydrazide (5 mmol, 1.20 g) in methanol (20 mL) and the mixture was stirred at the refluxing temperature for 4 h, after which the solvent was removed in vacuo. The white product was washed with cold methanol and dried in vacuo. Yield: 75%. ^{1}H NMR (400MHz, DMSO-d$_6$) δ 9.28 (s, 1H), 8.49(d, J=4.61, 1H), 7.81(d, J=2.51, 1H), 7.78(d, J=7.69, 1H),7.71(t, 2H), 7.43(m, 1H), 7.38(d, J=7.52, 2H), 7.30(dd, 1H),7.24(t, 1H), 7.07(d,J=8.35, 1H), 6.96(t, 1H), 6.75(d, J=8.25, 1H), 6.70(t, 1H), 6.36(d, J=2.49, 1H), 3.81(s, 3H) ppm.

Preparation of ligand 2-(3-methoxyphenyl)-3-((pyridin-2-ylmethylene)amino)-2,3-dihydraquinazolin-4(1H)-one, [pq-3OCH$_3$]: The white solid was obtained in the similar manner to that of **pq-2OCH$_3$** except that 3-methoxybenzaldehdye was used instead of 2-methoxybenzaldehdye. Yield: 73%. ^{1}H NMR

(400MHz, DMSO-d$_6$) δ 8.84 (s, 1H), 8.49(d, J=4.93, 1H), 7.90(d, J=3.81, 1H), 7.79(d, J=7.09, 1H), 7.70(t, 1H), 7.40(d, J=7.88, 1H), 7.33(t, 1H), 7.29(m, 1H),7.24(d, J=7.95, 3H), 6.99(d, J=6.67, 1H), 6.77(d, J=8.25, 1H), 6.71(t, 1H), 6.48(d, J=3.11, 1H), 3.76(s, 3H)ppm.

Caution! *Perchlorate salts are potentially explosive in organic solvent, only small amount should be treated with caution.*

Preparation of compound [Fe(pq-2py)$_2$](ClO$_4$)$_2$·CH$_3$OH·2H$_2$O (1): A solution of Fe(ClO$_4$)$_2$· 6H$_2$O (0.05 mmol, 0.0181 g) in MeOH (6 mL) was added to a solution of pq-2py (0.1 mmol, 0.0329 g) in 10 mL MeOH / CH$_3$CN (v:v, 4:6). The resulting dark-red mixture was stirred under nitrogen atmosphere for 1 h. The suspension was then filtered and the filtrate was diffused with diethyl ether. Dark red block-shaped single crystals suitable for X-Ray diffraction analysis were obtained after several days. Yield: 48% (based on Fe). IR(KBr pellet, cm^{-1}): 499(w), 518(w), 542.40(w), 627 (m), 696 (w), 754 (m), 845 (w), 893 (w), 927 (w), 999 (w), 1100 (s), 1153 (s), 1225 (m), 1307 (w), 1346 (w), 1375 (w), 1408 (m), 1452 (m), 1519 (w), 1611 (s), 3055(w), 3325 (m). Anal. Calcd for Fe(C$_{19}$H$_{15}$N$_5$O)$_2$·(ClO$_4$)$_2$·(CH$_4$O)·(H$_2$O)$_2$: H, 3.90; C, 47.72; N, 14.27. Found: H, 3.78; C, 47.75; N, 14.37. The sample **1** was then subject to dry at room temperature under vacuum for 4 days to prepare the fully desolvated sample **1-des**. Anal. Calcd for Fe(C$_{19}$H$_{15}$N$_5$O)$_2$·(ClO$_4$)$_2$: H, 3.31; C, 49.97; N, 15.33. Found: H, 3.73; C, 49.05; N, 15.41.

Preparation of compound [Fe(pq-2py)$_2$](BF$_4$)$_2$·2CH$_3$CN·1.75H$_2$O (2): The dark red block-shaped crystals of complex **2** suitable for X-ray diffraction were obtained in the similar manner to that described for complex 1 except that Fe(BF$_4$)$_2$·6H$_2$O was used instead of Fe(ClO$_4$)$_2$· 6H$_2$O. Yield: 42% (based on Fe). IR (KBr pellet, cm^{-1}): 537 (w), 619 (w), 7008(w), 754 (s), 845 (w), 893 (w), 1076 (s), 1154(m), 1225 (m), 1308(w), 1375 (w), 1413 (m), 1452 (m), 1514 (w), 1611 (s), 3373 (m). Anal. Calcd for Fe(C$_{19}$H$_{15}$N$_5$O)$_2$·(BF$_4$)$_2$·(C$_2$H$_3$N)$_2$·(H$_2$O)$_{1.75}$: H, 3.97; C, 50.35; N, 16.78. Found: H, 4.41; C, 50.65; N, 17.06. The sample **2** was then subject to heat treatment at 150 $^{\circ}$C for 4 hours under vacuum to obtain the fully desolvated sample **2-des** based on the analysis of TGA. Anal. Calcd for Fe(C$_{19}$H$_{15}$N$_5$O)$_2$·(BF$_4$)$_2$: H, 3.40; C, 51.39; N, 15.77. Found: H, 3.86; C, 51.05; N, 15.68.

Preparation of compound [Fe(pq-2py)$_2$](CF$_3$SO$_3$)$_2$·CH$_3$CN·CH$_3$OH (3): The dark red crystals of complex **3** suitable for X-ray diffraction were obtained by following the same procedure as that described for complex **1** except that Fe(CF$_3$SO$_3$)$_2$·2CH$_3$CN was used instead of Fe(ClO$_4$)$_2$· 6H$_2$O. Yield: 52% (based on Fe). IR (KBr pellet, cm^{-1}): 518(w), 546 (w), 575 (w), 643 (m), 701(w), 754 (m), 845 (w), 889(w), 989 (w), 1028 (s), 1167 (s), 1245 (s), 1278 (s), 1346 (w), 1379 (w), 1413 (m) , 1452 (m), 1509 (m), 1567 (w), 1611 (s), 3046 (w), 3469 (m), 3571(m). Anal. Calcd for Fe(C$_{19}$H$_{15}$N$_5$O)$_2$·(CF$_3$SO$_3$)$_2$·(C$_2$H$_3$N)·(CH$_4$O): H, 3.43; C, 47.56; N,14.19. Found: H, 3.23; C, 47.65; N, 13.82. The desolvated sample **3-des** sample was obtained in the similar manner to that of **2-des**. Anal. Calcd for Fe(C$_{19}$H$_{15}$N$_5$O)$_2$·(CF$_3$SO$_3$)$_2$: H, 3.90; C, 47.72; N, 14.27. Found: H, 3.53; C, 47.39; N, 14.42.

Preparation of compound [Fe(pq-2OCH$_3$)$_2$](ClO$_4$)$_2$·H$_2$O (4): The dark red block-shaped crystals of complex **4** suitable for X-ray diffraction were obtained in the similar manner to that described for complex **1** except that pq-2OCH$_3$ was used instead of pq-2py. Yield: 73% (based on Fe). IR (KBr pellet, cm^{-1}): 504(w), 532 (w), 626 (m), 691 (w), 754 (m), 845 (w), 888 (w), 932 (w), 985(w), 1023 (w), 1100 (s), 1154(m), 1227 (m), 1245 (m), 1308(w), 1356(w), 1408 (m), 1447 (m), 1490 (m), 1529 (m), 1569 (m), 1609 (s), 2838 (w), 2949 (w), 3055 (w), 3339 (m). Anal. Calcd for Fe(C$_{21}$H$_{18}$N$_4$O$_2$)$_2$·(ClO$_4$)$_2$·(H$_2$O): H, 3.87; C, 50.98; N, 11.32. Found: H, 3.57; C, 51.43; N, 11.09. The desolvated sample **4-des** was obtained in the similar manner to that of **1-des**. Anal. Calcd for Fe(C$_{19}$H$_{15}$N$_5$O)$_2$(ClO$_4$)$_2$: H, 3.73; C, 51.92; N, 11.53. Found: H, 3.82; C, 52.05; N, 11.22.

Preparation of compound [Fe(pq-3OCH$_3$)$_2$](ClO$_4$)$_2$·H$_2$O (5) : The dark red block-shaped crystals of complex **5** suitable for X-ray diffraction were obtained in the similar manner to that described for complex **4** except that pq-3OCH$_3$ was used instead of pq-2OCH$_3$. Yield: 70% (based on Fe). IR (KBr pellet, cm^{-1}): 507 (w), 536 (w), 626(m), 694 (w), 750 (m), 775.33(w), 864 (w), 889 (w), 920(w), 981 (w), 1097 (s), 1155 (m), 1226 (m), 1261 (w), 1305 (w), 1350 (w), 1371 (w), 1409 (m), 1452 (m), 1488 (m), 1523 (m), 1610 (s), 2837 (w), 2962 (w), 3503 (w), 3342 (m). Anal. Calcd for Fe(C$_{21}$H$_{18}$N$_4$O$_2$)$_2$·(ClO$_4$)$_2$·(H$_2$O): H, 3.87; C, 50.98; N, 11.32. Found: H, 3.76; C, 50.44; N, 11.09. The desolvated sample **5-des** was obtained in the similar manner to that of **1-des**. Anal. Calcd for Fe(C$_{19}$H$_{15}$N$_5$O)$_2$(ClO$_4$)$_2$: H, 3.73; C, 51.92; N, 11.53. Found: H, 3.92; C, 52.34; N, 11.84.

X-ray Crystallography

The crystal data for all the complexes at the selected temperature have been collected on a Bruker SMART CCD diffractometer (Mo Kα radiation, λ = 0.71073 Å). SMART was used for collecting frames of data, indexing reflections, and determining lattice parameters, SAINT for integration of the intensity of reflections and scaling, SADABS for absorption correction, and SHELXTL for space group and structure determination and least-squares refinement on F^2.[45] All structures were determined by direct methods using SHELXS and refined by full matrix least-squares methods against F^2 with SHELXL.[46] All of the non-hydrogen atoms except the disordered solvent molecules were refined with anisotropic thermal displacement coefficients. Hydrogen atoms were located geometrically, whereas those of solvent molecules were found on Fourier difference maps, and all of the hydrogen atoms were refined in riding mode. Because of weak diffraction and disordered solvents molecules in the lattice, the SQUEEZE function of PLATON was applied for complexes **1**-120K, **1**-296K, **2**-100K, **2**-180K and **3**-200K. The residual electron counts were 182 e$^-$, 137 e$^-$, 197 e$^-$, 198 e$^-$ and 143 e$^-$ per unit cell, respectively, corresponding to the missing solvent molecules,[47] which is in accordance with those calculated from TGA and elemental analysis data (Figure S13, Figure S14). Parameters for data collection and refinement of the compounds are summarized in Table 1. It should be noted that the data were of poor quality but sufficient to confirm connectivity.

ARTICLE

Table 1. Crystallographic Data for **1-5**.

	1		2		3	4		5
T (K)	120	296	100	180	200	100	296	296
Formula	$C_{38}H_{30}N_{10}O_{10}Cl_2Fe$		$C_{38}H_{30}N_{10}O_2B_2F_8Fe$		$C_{40}H_{30}O_8N_{10}S_2F_6Fe$	$C_{42}H_{34}N_8O_{13}Cl_2Fe$		$C_{42}H_{34}N_8O_{12}Cl_2Fe$
MW(g/mol)	913.47		888.19		1012.71	985.52		969.52
Crystal system	Triclinic		Triclinic		Triclinic	Orthorhombic		Orthorhombic
Space group	$P\bar{1}$		$P\bar{1}$		$P\bar{1}$	F_{dd2}		F_{dd2}
Z	2		2		2	8		8
a[Å]	11.988(4)	11.801(6)	11.8910(19)	11.893(3)	11.8477(19)	33.209(4)	33.402(6)	32.579(10)
b[Å]	12.347(4)	13.315(6)	12.235(2)	12.353(3)	14.823(2)	14.8798(18)	15.304(3)	17.101(4)
c[Å]	18.255(5)	17.303(8)	18.064(3)	18.068(5)	16.192(4)	18.8479(18)	19.044(3)	18.604(4)
α[°]	72.264(7)	110.308(11)	72.999(4)	73.665(5)	104.000(5)	90	90	90
β[°]	74.636(7)	91.184(12)	75.187(3)	75.689(5)	98.380(5)	90	90	90
γ[°]	86.982(8)	104.924(12)	86.189(3)	86.462(5)	113.241(4)	90	90	90
V[Å^3]	2480.4(13)	2445.6(19)	2429.6(7)	2468.1(10)	2440.7(8)	9313.6(19)	9734(3)	10365(5)
$\rho_{calc.}$(g/cm^3)	1.223	1.240	1.214	1.195	1.378	1.406	1.339	1.243
F(000)	936	936	904	904	1032	4048	4037	3984
$R_1{}^a$(I>2σ(I))	0.1070	0.1351	0.1105	0.0962	0.1121	0.0961	0.0911	0.0958
$wR_2{}^b$ (I>2σ(I))	0.2343	0.3517	0.2841	0.2812	0.3086	0.2473	0.2336	0.2304
R_1(all data)	0.1828	0.2083	0.0883	0.1297	0.1651	0.1398	0.1077	0.2022
wR_2(all data)	0.2631	0.3400	0.2567	0.3096	0.3498	0.2876	0.2491	0.3048
GooF	1.058	1.099	1.086	1.081	1.083	1.033	1.017	0.966

$^a R_1 = \Sigma||F_o| - |F_c||/\Sigma|F_o|.$ $^b wR_2 = \{\Sigma[w(F_o^2 - F_c^2)^2]/\Sigma[w(F_o^2)_2]\}^1$

Results and discussion

Structure Analysis

The 2-substituent dihydroquinazoline ligands **pq-R** were synthesized through ring-closure reaction of the corresponding aldehyde and 2-amino-N'-((pyridin-2-yl)methylene) benzohydrazide following modified literature procedures (Scheme 1).[41] The metal complexes were formed by treatment with a MeOH/CH$_3$CN mixed solution containing 2 equiv each of **pq-R** and 1 equiv of Fe(II) salts to give a dark red solution under nitrogen atmosphere. The dark-red crystals, [Fe(**pq-R**)$_2$](X)$_2$·xCH$_3$OH·yCH$_3$CN·zH$_2$O(R = 2-py: X = ClO$_4$$^-$, x=1, y=0, z=2 (**1**); BF$_4$$^-$, x=0, y=2, z=1.75 (**2**); CF$_3$SO$_3$$^-$, x=1, y=1, z=0(**3**); and X = ClO$_4$$^-$: R = 2-OCH$_3$, x=0, y=0, z=1(**4**); R = 3-OCH$_3$, x=0, y=0, z=1 (**5**)) suitable for X-ray diffraction were obtained by subsequently carefully diffusing diethyl ether vapor into this solution. The most obvious feature in the IR spectra of the iron compounds is the presence of the absorptions of the perchlorate counter ion [v(ClO$_4$$^-$): ~1100 cm^{-1} (very strong), ~627 cm^{-1} (medium intensity)] for **1**. As expected, the perchlorate complexes **4** and **5** exhibit characteristic v(ClO$_4$$^-$) absorptions in their spectra. The imine C=N bond is indicated by the vibrational bands in the range 1598–1636 cm^{-1}. The keto C=O bond is indicated conspicuously by the characteristic intense absorptions at the band ~1600 cm^{-1} for all the Fe(II) complexes. The characteristic N-H vibrational absorptions appear in the ranges ~1350-1490 cm^{-1} for the dihydroquinazoline backbone, further confirmed the components of the complex. To our best knowledge,

complexes **1**-**5** represent the first examples of Fe^{II} complexes of dihydroquinazoline derivative.

Single-crystal X-ray diffraction analyses for the selected compounds were carried out at both high and low temperature. At higher temperature, complexes **1-3** crystallize in the triclinic space group $P\bar{1}$ and are isostructural to one another (Table 1). However, complexes **4** and **5** crystallize in the orthorhombic F_{dd2} space group and the ligands are crystallographically identical. A perspective view of the molecular structure of **1** and **4** is shown in Fig. 1. The iron(II) ion is hexa-coordinated by two tridentate Schiff base ligands with the carbonyl O, azomethine N and pyridine N as donor atoms, forming cation iron complex. At high temperature, the average Fe−N$_{py}$, Fe−N$_{azo}$, and Fe−O distances across the series **1-3** fall in the ranges of 2.157(6)−2.171(8), 2.122(4)−2.137(6), and 2.098(6)−2.119(4) Å, respectively, which is consistent with the presence of high-spin S = 2 Fe^{II} centers (Table 2).

At low temperature, crystals of **1-3** maintain their space group of $P\bar{1}$, albeit without significantly decrease in unit cell dimensions relative to the high temperature data (Table 1). The average Fe−N$_{py}$/ Fe−O bond distances exhibit only a little change, i.e., 2.164(7) / 2.130(5), and 2.153(4) / 2.121(3) Å, together with the Fe−N$_{azo}$ of 2.091(7) and 2.115(4) Å for **1** and **2**, respectively (Table 2), indicative of the slight change of the octahedron sphere around Fe(II) center. Compared to the work by Gao et al,[35] the Fe-N$_{azo}$ bond distance is comparable, the Fe−N$_{py}$ distance became *ca.* 0.06 Å shorter and Fe-O is about 0.04 Å longer. Within the dihydroquinazoline group in **1**, the C-N bond distance involving C7-N3 and C5-N1 is 1.359(9) and 1.358(10) Å together with N8−C26 and N6−C27 bond

Table 2. Selected Interatomic Distances (Å) and Angles (deg) for **1-5**.

	1		2		3	4		5
T(K)	120	296	100	180	200	100	296	296
Fe-N$_{py}$	2.147(7)	2.162(7)	2.145(4)	2.152(5)	2.151(5)	2.137(9)	2.141(8)	2.148(11)
	2.181(6)	2.179(8)	2.1613)	2.172(4)	2.162(6)	2.137(9)	2.141(8)	2.148(11)
Fe-N$_{py, avg}$	2.164(7)	2.171(8)	2.153(4)	2.162(5)	2.157(6)	2.137(9)	2.141(8)	2.148(11)
Fe-N$_{azo}$	2.079(7)	2.137(6)	2.115(4)	2.119(4)	2.123(6)	2.125(9)	2.137(7)	2.123(10)
	2.103(6)	2.137(6)	2.115(4)	2.124(4)	2.139(6)	2.125(9)	2.138(7)	2.123(10)
Fe-N$_{azo, avg}$	2.091(7)	2.137(6)	2.115(4)	2.122(4)	2.131(6)	2.125(9)	2.138(7)	2.123(10)
Fe-O	2.108(5)	2.094(6)	2.099(3)	2.099(4)	2.114(5)	2.121(6)	2.125(6)	2.160(8)
	2.151(5)	2.104(6)	2.143(3)	2.138(4)	2.122(5)	2.121(6)	2.125(6)	2.160(8)
Fe-O$_{avg}$	2.130(5)	2.098(6)	2.121(3)	2.119(4)	2.118(5)	2.121(6)	2.125(6)	2.160(8)
Σ^d	147.2(3)	149.3(3)	147.4(12)	147.8(15)	151.1(2)	152.2(3)	157.6(3)	165.2(4)

distances of 1.371(10) and 1.376(11) Å, respectively, are intermediate between the normal C−N double bond and single bond. In contrast, the C13−N1 and C13−N3 together with C38−N6 and C38−N8 bond distances are in the range of 1.424(10)−1.486(9) Å, which is typical for a usual C−N single bond. These collective distances suggest that **pq-2py** ligand is partially conjugated upon binding to Fe(II). Furthermore, the C−O bond varies from 1.239(8) to 1.254(9) Å, suggesting the normal double bond. Hence, these distances are consistent with Fe^{II} center being ligated by an oxygen atom of a carbonyl group and a nitrogen atom of a neutral imine group, such that **pq-2py** ligand is best described as a neutral carbohydrazone derivative upon coordination to Fe(II) center.[48]
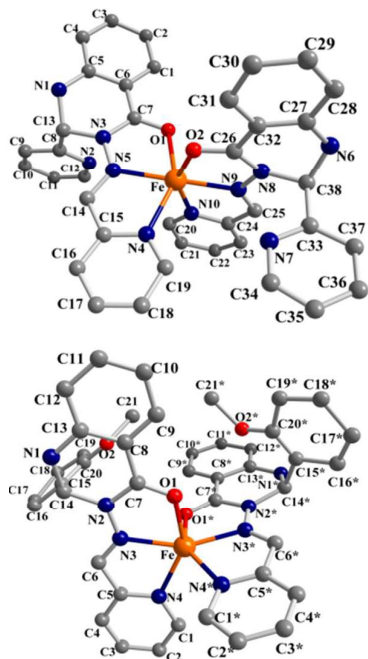
This distortion from an ideal octahedron can be quantified through the parameter Σ,[49] which is defined as the sum of the absolute deviations of each of the 12 cis-disposed L−Fe−L angles from 90°. In general, the spin crossover will induce the change of Σ with small Σ in the LS state and larger Σ in the HS state.[50] Analysis of the Fe centers in **1** with SCO phenomenon at the temperature before and after transition gives values of Σ = 149.3(3)^o and 147.2(3)^o, respectively. The Σ analysis for **2** revealed less difference between high- and low-temperature data and are indicative of high portion of HS Fe(II) in this system.
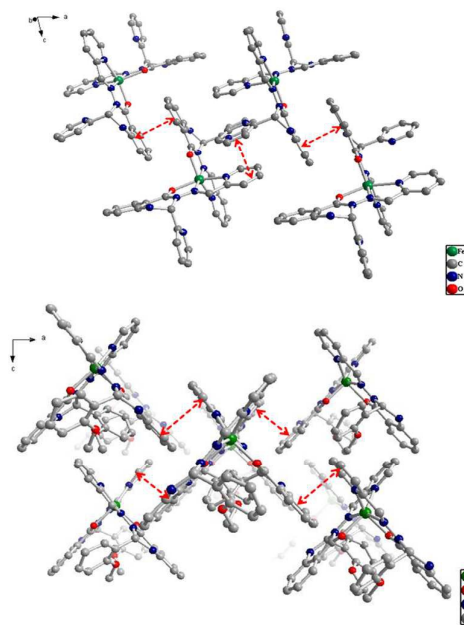

Figure. 1 Molecular structure of **1** at 120 K (top) and **4** at 100 K(bottom). (hydrogen atoms, anions and solvent molecule are omitted for clarity). Symm. code: *: -x+1/2, -y+5/2, z.

Figure 2. Crystal packing portion of the crystal structure of **1** (120 K, top) and **4** (100 K, bottom) at, as viewed along the crystallographic *b* axis, highlighting the abundant intermolecular π…π stacking.

Along these lines, the average Fe−N$_{py}$ bond distances in **4** between high and low-temperature structure are quite similar, and both the average Fe-N$_{azo}$ and Fe-O showed the slight change from 2.138(7) Å to 2.125(9) Å and from 2.125(6) Å to

2.21(6) Å, respectively, suggesting a majority of high-spin Fe^{II} centers in **4** at 100 K.

Table 3. The observed π…π stacking mode in compounds **1-5**.

Compound	1	2	3	4	5
π…π stacking	centroid…centroid distance (Å)				
Ring A…Ring A[a]	3.554	3.486	3.400	-	-
Ring B[b]…Ring C[c]	3.463	3.342	3.819	-	-
Ring A…Ring B	-	-	-	3.446	3.529

[a] Ring A denotes dihydroquinazoline group; [b] Ring B denotes coordinated pyridyl ring; [c] Ring C denotes free pyridyl or substituent phenyl ring; -: not observed.

Overall, the 2+ charge of each cation complex is balanced by two noncoordinating counteranions. These bulky anions interact with the Fe^{II} cations through X…H−N hydrogen-bonding interactions, evident from contacts of acceptor(anion)…donor(N) on dihydroquinazoline groups with the shortest intermolecular anion···N distances of 2.864, 2.990 and 3.050 Å for **1**, **2** and **3** at high temperature, respectively. The presence of such bulky anions engenders a large separation between Fe^{2+} complexes in the solid state, with the shortest intermolecular Fe···Fe distances in the range of 9.777(4)−9.782(4) Å at 296 K and 9.565(4)−9.662(4) Å at 100 K. Most importantly, in the crystal packing each molecule interacts with the adjacent iron complexes *via* π…π stacking of the coordinated pyridyl and free pyridyl groups with the centroid…centroid distance of 3.463 Å for complex **1**(Figure 2). In addition, the stabilization of an infinite three-dimensional network was also supported by the intermolecular π…π stacking *via* two dihydroquinazoline groups with the centroid…centroid distance of 3.554 Å. The similar π…π stacking interactions were found to exist in the packing structure of **2** and **3**. Compared with the homologous compound **1**, the different stacking style was presented in another homologue **4**, namely, only one type of intermolecular π…π stacking interlinked the coordinated pyridyl and dihydroquinazoline group with the centroid…centroid distance of 3.446 Å for **4** and 3.529 Å for **5** (Figure 2, bottom and Figure S11), respectively. Hence, the different mode of intermolecular interactions between **1-3** and **4-5** series should enable the electronic effects on spin crossover with cooperative interactions that are likely to be different between them.(Table 3) However, in the closely related work,[35] hydrogen-bond interaction rather than π…π stacking, which is the possible source of cooperative interaction, occurring between terminal O atom and azomethine N atom is found in the crystal packing of solvated crystal, leading to an infinite two-dimensional network.

Magnetic Properties

Magnetic susceptibility measurements were performed on the freshly prepared samples of **1–5**, in the temperature range 5–300 K, under an applied magnetic field of 2500 G (see Figure 3 and Figure S12). Both **1** and **2** are high-spin at room temperature and undergo incomplete spin-transitions upon cooling, **3** is almost high-spin over the temperature range ($\chi_M T$ = 3.26 cm^3 mol^{-1} K) between 45–300 K (Figure 3(a)). As the temperature is decreased, $\chi_M T$ values of **1** and **2** initially remain constant before undergoing gradual and slight decline.

Although the S-shaped $\chi_M T$ curve is a signature of spin crossover, the non-zero minimum values of $\chi_M T$ at low temperature indicate that a considerable portion of high-spin Fe^{II} centers [90(1), 87(1) and 93(1)% of Fe^{II} centers for **1**, **2** and **4**, respectively], which is consistent with the X-ray diffraction analysis. The low temperature decrease in $\chi_M T$ below 45 K is not evidence of further spin-transition, but is caused by zero-field splitting of the high-spin manifold. The incompleteness is likely caused by an inherent structural impossibility for the compound to achieve a pure spin state in which all metallic centres are LS, which is possibly affected by the solvent loss. Indeed, samples which have been desolvated by heat treatment under vacuum based on the TG results exhibit increasing percentages of transition centres(Figure S13, S14). Despite that the solvate sample showed little spin crossover, however, upon solvent loss, the transition percentage varies across the **1-3** series in the order of BF_4^-(82%) > ClO_4^-(54%) > $CF_3SO_3^-$(7%)(Figure 3(b)). It's worthy to note that the slope of the curve practically unchanged between **1** and **2**. Hence, the cooperativity seems to be unaffected by anion changes between BF_4^- and ClO_4^-. Finally, in order to further investigate the substituent effect on spin transition, the compounds **4** and **5** were prepared and their magnetic data were analyzed, the compound **5** is basic high-spin within the whole temperature region and only a small decreased portion of $\chi_M T$ product at 100 K, but compound **4** exhibits the onset of a gradual spin-transition on continuous cooling over a wide temperature range from 220 K to 95 K, implying it is only tiny SCO completeness.(Figure S12)
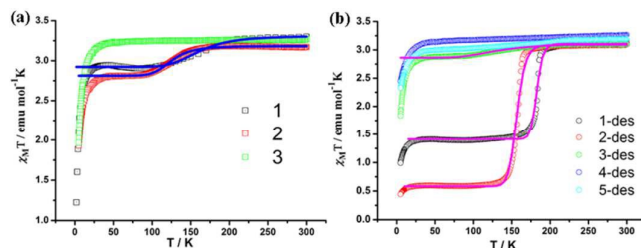

Figure 3. (a) Plots of $\chi_M T$ versus T for compounds **1** (ClO_4^-, black), **2** (BF_4^-, red), **3** ($CF_3SO_3^-$, green) and (b) their corresponding desolvated samples which were subject to heating at 150 °C for 4 hours under vacuum prior to magnetic measurement. Circles represent experimental data, whereas solid lines correspond to fits based on a domain model as described in the text. Note: All the measurements were undertaken in sweep mode at scanning rate of 1 K/min.

In some cases, the SCO completeness is to a certain extent dependent on the cooling rate.[51-55] Samples which have been rapidly cooled usually exhibit lower percentages of transition centres, while slowly cooled samples show higher values. Accordingly, if the temperature is kept at 120 K for about 24 h in the SQUID holder, only a negligible decrease of the $\chi_M T$ value is detected on complex **1**. Hence, the incompleteness observed for compound **1** is independent of the cooling rate. A change of bonding distance around metal center occurring during the transition may also justify this incompleteness as seen for compound **1**. Unfortunately, we could not collect high-quality diffraction data of desolvated samples due to the

crystal collapse subject to loss of lattice solvent despite many attempts, and therefore the crystal structures of desolvated complexes **1** and **2** could not be obtained.

o estimate the relevant thermodynamic parameters associated with the spin transition, we have fitted the experimental data between 50 K and 300 K using the domain model (eq 1).[42,56]

$$\ln \frac{(1-\gamma_{HS})}{\gamma_{HS}} = \frac{n\Delta H}{RT} - \frac{n\Delta S}{R} \qquad (1)$$

The HS molar fraction, n_{HS}, can be expressed as a function of the magnetic susceptibility through (eq 2) where ΔH and ΔS are the enthalpy and entropy parameters, R is the universal gas constant, and n is the domain size and represents the number of molecules per domain. The fit of the magnetic data were performed by use of the program Origin 6.1 from OriginLab Corporation.

$$\gamma_{HS} = \frac{[(\chi_M T)_{exp} - (\chi_M T)_{LS}]}{[(\chi_M T)_{HS} - (\chi_M T)_{LS}]} \qquad (2)$$

where $(\chi_M T)_{exp}$ is the value of $\chi_M T$ at any temperature and $(\chi_M T)_{LS}$ and $(\chi_M T)_{HS}$ correspond to the pure LS and HS states, respectively. In the present case, we have considered that the spin conversion is incomplete at low temperature, hence, $(\chi_M T)_{LS}$ is an adjustable parameter and that $(\chi_M T)_{HS}$ is the value at room temperature.

The temperature dependence of the HS molar fraction (γ) could be fitted with the domain SCO model to give the enthalpic and entropic thermodynamic parameters for all the solvated samples, which are quite reasonable when compared with those previously reported for Fe[II] spin crossover complexes (using the above model with domain size parameter n = 1); However, the fit of the desolvated sample **1-des** according to the domain SCO model gave rise to the thermodynamic parameters n·ΔH = 63.96 kJ mol^{−1} and n·ΔS = 349.58 J mol^{−1} K^{−1}. Taking into account that typical ΔS values for Fe(II) SCO complexes lie in the range of 40–65 J mol^{−1} K^{−1},[57] the n parameter appears to be within 6-8. The similar model produced the fitting parameters for **2-des** sample as following: nΔH = 37.3(4) kJ/mol and thus nΔS = 237.8(3) J/K/mol with n = 4 or 5. The substantial domain size is also reflected by the relative abruptness of the SCO conversion curve; the transition for **1-des** and **2-des** is clearly more abrupt than expected for a simple two state Boltzmann distribution. Least-squares fitting also produced the anion-dependent crossover temperatures ($T_{1/2}$) in the order of $T_{1/2}(ClO_4^-) > T_{1/2}(BF_4^-) > T_{1/2}(SO_3CF_3^-)$ for the solvent-free samples (see Table 4).[58,59] Alternatively, the degree of completeness (in the desolvated samples) seems to be correlated to the anion size, i.e., $CF_3SO_3^- > ClO_4^- > BF_4^-$. An effect of the counteranion on the spin crossover properties concerns the remaining fraction of HS species at low temperatures, which is 93% for **3-des** ($CF_3SO_3^-$), 46 % for **1-des** (ClO_4^-) and 18 % for **2-des** (BF_4^-) in order. Such behaviour has been observed in a few cases,[31,59,60] where it was explained by larger steric interactions close to the metal center that stabilise the HS state.

Table 4. Summary of Parameters Obtained from Fits to Magnetic Data[a]

	nΔH (kJ/mol)	nΔS (J/mol·K)	$T_{1/2}$ (K)	n	γ_{HS}(%)
1	9.87	61.12	161.4(7)	1	90
1-des	63.96	349.58	182.9(6)	6-8	46
2	9.84	78.72	125.0(0)	1	87
2-des	37.34	237.83	157.0(8)	4-5	18
3-des	4.63	33.48	138.3(5)	1	93

[a] Fits obtained using a domain model as described in the text.

With regard to the SCO magnetic data, it seems obscure to evaluate the influence factors of N_4O_2 SCO compounds in the related work. Complete and room temperature spin transition was obtained in a mononuclear Fe(II) spin crossover compound employing 2-hydraxy-3-methyl-N'-((pyridin-2-yl)-ethylidene) benzohydrazide as ligand (Scheme 1).[36] In another example by the same authors, the compounds exhibit the similar SCO behavior, however, the critical temperature was significantly decreased by the desolvation from 310 K to 280 K and the completeness showed the negligible change upon desolvation.[35] The type of the carbohydrazone Schiff-base ligands often undergo metal- or base-assisted tautomerisation, which influenced the spin state and valence of iron ion in the recent work.[37] However, it is anticipated that N_4O_2 donor system behaves differently with regard to ligand field giving rise to the spin transition.

Mössbauer spectroscopy

To further investigate the spin crossover in this system, the selected [57]Fe Mössbauer spectra of the desolvated complex **1-des** and **2-des** were recorded at temperature before and after spin transition, i.e. 293 and 100 K, respectively (Figure 4). At 293 K, the Mössbauer spectrum of **1-des** exhibits a wide quadrupole doublet with a quadrupole splitting (QS) of 2.492 and an isomer shift (IS) of 0.819 mm s^{−1}, showing a typical HS state. On cooling to 100 K, a narrow quadrupole doublet appears and gains in intensity at the expense of the original HS doublet. The peak with QS=0.817 and IS=0.201 mms[−1] can be assigned to LS Fe[II] arising from the thermally induced spin transition. The original doublet signal corresponding to the HS state becomes slightly wider with QS=2.857 and IS=0.971 mms[−1]. Additionally, the low/high-spin relative fraction in the Mössbauer results is consistent with that of magnetic data (Table 5). The spectra of complex **2-des** at 293 K exhibits a doublet with the quadrupole splitting 2.297 mms[−1] and isomer shift 0.816 mms[−1] characteristic of a high spin iron(II) centre. Mössbauer spectroscopy detected a low spin (LS) iron(II) in the sample of **2-des** by the presence of a poorly resolved quadrupole-split doublet (QS = 0.576 mms[−1], IS = 0.112 mms[−1]), [Fig. 4(b)] indicating the existence of low-spin population even at room temperature. On lowering the temperature to 100 K, the resonance lines start to broaden and the intensity of the LS doublet increases at the expense of HS doublet, confirming thermally induced HS → LS conversion for a single Fe(II) site. Surprisingly, the portion of LS state from Mössbauer data is clearly lower than that from the magnetic data, which perhaps arises from the partial rehydration of the dry sample, **2-des**, under ambient condition. Hence, the variation of the relative

New Journal of Chemistry Accepted Manuscript

ARTICLE

fraction of both doublets (corresponding to HS and LS species) with the temperature clearly confirms the incomplete spin crossover.

Table 5. Parameters of Mössbauer spectra for **1-des** and **2-des**.

	T/K	IS	QS	Γ	Fraction(%)	State
1-des	293	0.819	2.492	0.338	100	HS
	100	0.971	2.857	0.700	47	HS
		0.201	0.817	0.836	53	LS
2-des	293	0.816	2.297	0.460	84	HS
		0.112	0.576	0.573	16	LS
	100	0.914	2.716	0.614	35	HS
		0.205	0.797	0.720	65	LS

Note: IS: isomer shift (mms^{-1}, with reference to metallic iron at 293 K), QS is quadrupole splitting (mms^{-1}), Γ: Line width (mm s^{-1}).
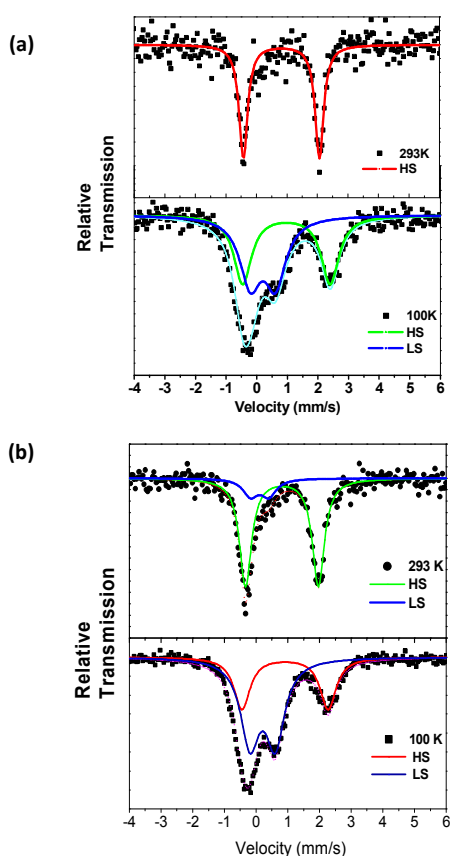

Figure 4. Zero-field Mössbauer spectra for crystalline samples of **1-des** (a) and **2-des** (b) at selected temperatures. Black squares represent experimental data. Colored solid lines correspond to individual components of the overall fits assigned to Fe$_{HS}$, and the low-spin center in Fe$_{LS}$, respectively.

Conclusions

In conclusion, we demonstrated that the spin transition properties of a new family of dihydroquinazoline Fe(II) complexes. The modulation, including transition percentage and crossover temperature, in complexes of the isostructural compounds was influenced by subtle variation, such as solvent, the anion and ligand substituent. It has been widely recognized that the solvent effect is mainly related to the hydrogen bonding interaction. In our case, the transition percentage is lifted upon erasing hydrogen bonding. As to ClO$_4^-$ and BF$_4^-$, two anions have some similarities in a tetrahedral configuration, involving hydrogen-bonding interaction, and often falling in disorder. Indeed, both the ClO$_4^-$ and BF$_4^-$ derivatives show similar slopes in the plot of χ_MT versus T with large degrees of cooperativity in the dry samples. Their differences lie mainly in the aspects of size and electronic properties. In our study, the striking differences are found in the transition percentage by the change of counteranion. Substituent groups play crucial role in varying the intermolecular π…π stacking interactions, which is regarded as the source of cooperativity. Future efforts will take advantage of the chemical tunability of dihydroquinazoline derivatives to increase $T_{1/2}$ by further modifying both electronic and steric properties. In addition, we will seek to engender magnetic bistability in multinuclear spin crossover cluster through introduction of more coordination donors in an effort to introduce large degrees of cooperativity.

Acknowledgements

Notes and references

1 O. Kahn and C. Martinez, *Science,* 1998, **279**, 44.
2 P. Gutlich, A. Hauser and H. Spiering, *Angew. Chem. Int. Ed.*, 1994, **33**, 2024.
3 P. Gutlich, Y. Garcia and H. A. Goodwin, *Chem. Soc. Rev.,* 2000, **29**, 419.
4 M. A. Halcrow, *Chem. Soc. Rev.,* 2008, **37**, 278.
5 O. Sato, J. Tao and Y.-Z. Zhang, *Angew. Chem. Int. Ed.,* 2007, **46**, 2152.
6 M. Sy, F. Varret, K. Boukheddaden, G. Bouchez, J. Marrot, S. Kawata and S. Kaizaki, *Angew. Chem. Int. Ed.,* 2014, **53**, 29.
7 G. A. Craig, O. Roubeau and G. Aromi, *Coord. Chem. Rev.,* 2014, **269**, 13.
8 M. Schmitz, M. Seibel, H. Kelm, S. Demeshko, F. Meyer and H. J. Kruger, *Angew. Chem. Int. Ed.,* 2014, **53**, 23.
9 R. Kulmaczewski, J. Olguin, J. A. Kitchen, H. L. C. Feltham, G. N. L. Jameson, J. L. Tallon and S. Brooker, *J. Am. Chem. Soc.,* 2014, **136**, 878.
10 R. W. Hogue, R. G. Miller, N. G. White, H. L. C. Feltham, G. N. L. Jameson and S. Brooker, *Chem. Commun*., 2014, **50**, 1435.
11 F. Habib, O. R. Luca, V. Vieru, M. Shiddiq, I. Korobkov, S. I. Gorelsky, M. K. Takase, L. F. Chibotaru, S. Hill, R. H. Crabtree and M. Murugesu, *Angew. Chem. Int. Ed.,* 2013, **52**, 11290.
12 W. Liu, X. Bao, L. L. Mao, J. Tucek, R. Zboril, J. L. Liu, FS. Guo, Z. P. Ni and M. L. Tong, *Chem. Commun.,* 2014, **50**, 4059.
13 J. A. Kitchen, J. Olguin, R. Kulmaczewski, N. G. White, V. A. Milway, G. N. L. Jameson, J. L. Tallon and S. Brooker, *Inorg.Chem*., 2013, **52**, 11185.
14 J. G. Park, I-R. Jeon and T. D. Harris, *Inorg. Chem*., 2015, **54**, 359.

15 E. Coronado, M. Gimenez-Marques, G. M. Espallargas, F. Rey and I. J. Vitorica-Yrezabal, *J. Am. Chem. Soc.,* 2013, **135**, 15986.

16 J. A. Kitchen, N. G. White, G. N. L. Jameson, J. L. Tallon and S. Brooker, *Inorg. Chem*., 2011, **50**, 4586.

17 M. M. Dirtu, A. Rotaru, D. Gillard, J. Linares, E. Codjovi, B. Tinant and Y. Garcia, *Inorg. Chem.,* 2009, **48**, 7838.

18 G. Dupouy, M. Marchivie, S. Triki, J. Sala-Pala, J. Y. Salaun, C. J. Gomez-Garcia and P. Guionneau, *Inorg. Chem*., 2008, **47**, 8921.

19 R. Pritchard, S. A. Barrett, C. A. Kilner and M. A. Halcrow. *Dalton Trans*., 2008, 3159.

20 M. Mitsumi, S. Ohtake, Y. Kakuno, Y. Komatsu, Y. Ozawa, K. Toriumi, N. Yasuda, N. Azuma and Y. Miyazaki, *Inorg. Chem.,* 2014, **53**, 11710.

21 B. Gildea, M. M. Harris, L. C. Gavin, C. A. Murray, Y. Ortin, H. Muller-Bunz, C. J. Harding, Y. H. Lan, A. K. Powell and G. G. Morgan, *Inorg. Chem.,* 2014, **53**, 6022.

22 I. A. Gass, S. Tewary, G. Rajaraman, M. Asadi, D. W. Lupton, B. Moubaraki, G. Chastanet, J. F. Letard and K. S. Murray, *Inorg. Chem*., 2014, **53**, 5055.

23 B. Li, R. J. Wei, J. Tao, R. B. Huang, L. S. Zheng and Z. P. Zheng, *J. Am. Chem. Soc*., 2010, **132**, 1558.

24 X. Y. Chen, R. B. Huang, L. S. Zheng and J. Tao, *Inorg. Chem.,* 2014, **53,** 5246.

25 X. Y. Chen, H. Y. Shi, R. B. Huang, L. S. Zheng and J. Tao, *Chem. Commun*., 2013, **49**, 10977.

26 D. J. Harding, W. Phonsri, P. Harding, I. A. Gass, K. S. Murray, B. Moubaraki, J. D. Cashion, L. J. Liu and S. G. Telfer, *Chem. Commun*., 2013, **49**, 6340.

27 G. J. Halder, C. J. Kepert, B. Moubaraki, K. S. Murray and J. D. Cashion, *Science*, 2002, **298**, 1762.

28 Y. T. Wang, S. T. Li, S. Q. Wu, A. L. Cui, D. Z. Shen and H. Z. Kou, *J. Am. Chem. Soc*., 2013, **135**, 5942.

29 B. A. Leita, S. M. Neville, G. J. Halder, B. Moubaraki, C. J. Kepert, J. F. Letard and K. S. Murray, *Inorg. Chem*., 2007, **46**, 8784.

30 A. Galet, A. B. Gaspar, M. C. Munoz and J. A. Real, *Inorg. Chem*., 2006, **45**, 4413.

31 M. Quesada, F. Prins, E. Bill, H. Kooijman, P. Gamez, O. Roubeau, A. L. Spek, J. G. Haasnoot and J. Reedijk, *Chem. Eur. J.,* 2008, **14**, 8486.

32 D-Y. Wu, O. Sato, Y. Einaga and C-Y. Duan, *Angew. Chem. Int. Ed.,* 2009, **48**, 1475.

33 J. Tang, J. S. Costa, S. Smulders, G. Molnár, A. Bousseksou, S. J. Teat, Y. Li, G. A. van Albada, P. Gamez and J. Reedijk, *Inorg. Chem.,* 2009, **48**, 2128.

34 L. Zhang, G-C. Xu, H-B. Xu, V. Mereacre, Z-M. Wang, A. K. Powell and S. Gao, *Dalton Trans*., 2010, **39**, 4856.

35 L. Zhang, G-C. Xu, H-B. Xu, T. Zhang, Z-M. Wang, M. Yuan and S. Gao, *Chem. Commun.,* 2010, **46**, 2554.

36 L. Zhang, J.-J. Wang, G.-C. Xu, J. Li, D.-Z. Jia and S. Gao, *Dalton Trans*., 2013, **42**, 8205.

37 M. S. Shongwe, S. H. Al-Rahbi, M. A. Al-Azani, A. A. Al-Muharbi, F. Al-Mjeni, D. Matoga, A. Gismelseed, I. A. Al-Omari, A. Yousif, H. Adams, M. J. Morris and M. Mikuriya, *Dalton Trans.,* 2012, **41**, 2500.

38 (a) Z. Yu, T. Kuroda-Sowa, H. Kume, T. Okubo, M. Maekawa, and M. Munakata, *Bull. Chem. Soc. Jpn.* 2009, **82**, 333; (b) T. Kuroda-Sowa, K. Kimura, Jun. Kawasaki, T. Okubo, M. Maekawa, *Polyhedron*, 2011, **30**, 3189.

39 O. Lasco, E. Rivière, R. Guillot, M. B.-L. Cointe, J.-F. Meunier , A. Bousseksou and M-L Boillot, *Inorg. Chem.,* 2015, **54**, 1791.

40 K. S. Hagen, *Inorg. Chem.,* 2000, **39**, 5867.

41 MossWinn-Mössbauer spectrum analysis and database software. http://www.Mosswinn.com/.

42 O. Kahn, Molecular Magnetism; VCH: Weinheim, Germany, 1993.

43 R. Gup and B. Kırkan, *Spectrochimica Acta Part A.* 2005, **62**, 1188. H. Neuvonen, *J. Phys. Org. Chem.,* 2008, **21**, 173.

44 K. B. Gudasi, *Transit Metal Chem.,* 2005, **30**, 661.

45 *SMART and SAINT: Area Detector Control and Integration Software*; Siemens Analytical X-ray Systems, Inc.: Madison, WI, 1996.

46 *SHELXTL V5.1, Software Reference Manual*; Bruker, AXS, Inc.:Madison, WI, 1997.

47 (a) A. L. Spek, PLATON, *A Multipurpose Crystallographic Tool*; Utrecht University: Utrecht, The Netherlands, 1998. (b) A. L. Spek, *Acta Crystallogr.*, *Sect. D: Biol. Crystallogr.* 2009, **65**, 148.

48 (a) D. Wu, W. Huang, C. Duan, Z. Lin and Q. Meng, *Inorg. Chem.,* 2007, **46**, 1538. (b) D. Wu, W. Huang, Z. Lin, C. Duan, C. He, S. Wu and D. Wang, *Inorg. Chem.,* 2008, **47**, 7190.

49 P. Guionneau, M. Marchivie, G. Bravic, J.-F. Létard and D. Chasseau, *J. Mater. Chem.,* 2002, **12**, 2546. P. Guionneau, M. Marchivie, G. Bravic, J.-F. Létard and D. Chasseau, *Top. Curr. Chem*., 2004, **234**, 97 and references cited therein.

50 M. A. Halcrow. *Coordin. Chem. Rev.,* 2009, **253**, 2493.

51 N. Moliner, A. B. Gaspar, M. C. Muñoz, V. Niel, J. Cano and J. A. Real, *Inorg. Chem*., 2001, **40**, 3986.

52 V. A. Money, C. Carbonera, J. Elhaïk, M. A. Halcrow, J. A. K. Howard and J.-F. Létard, *Chem. Eur. J*., 2007, **13**, 5503.

53 J.-F. Létard, S. Asthana, H. J. Shepherd, P. Guionneau, A. E. Goeta, N. Suemura, R. Ishikawa and S. Kaizaki, *Chem. Eur. J*., 2012, **18**, 5924

54 N. Paradis, G. Chastanet, F. Varret and J.-F. Létard, *Eur. J. Inorg. Chem.,* 2013, 968.

55 D. Li, R. Clérac, O. Roubeau, E. Harté, C. Mathonière, R. Le Bris and S. M. Holmes, *J. Am. Chem. Soc.,* 2008, **130**, 252.

56 P. Atkins and J. De Paula, *Phys. Chem.*, Oxford University Press: Oxford, U.K., 2006, Chapter 5.

57 (a) O. Roubeau, M. Castro, R. Burriel, J. G. Haasnoot and J. Reedijk, *J. Phys. Chem. B* 2011, **115**, 3003. (b) Z. Arcis-Castíllo, S.Zheng, M. A. Siegler, O. Roubeau, S. Bedoui and S. Bonnet, *Chem. Eur. J.* 2011, **17**, 14826. (c) H. L. C. Feltham, C. Johnson, A. B. S. Elliott, K. C. Gordon, M. Albrecht and S. Brooker. *Inorg. Chem*., **2015**, **54**, 2902.

58 M. C. Muňoz and J. A. Real, *Coord Chem Rev.,* 2011, **255**, 2068.

59 G. J. Long, F. Grandjean and D. L. Reger, *Top. Curr. Chem*., 2004, **233**, 91.

60 M. Yamada, M. Ooidemizu, Y. Ikuta, S. Osa, N. Matsumoto, S. Iijima, M. Kojima, F. Dahan and J.-P. Tuchagues, *Inorg. Chem*., 2003, **42**, 8406.

New Journal of Chemistry Accepted Manuscript

Mononuclear spin-crossover complex from dihydraquinozoline derivatives were synthesized to enable the spin crossover phenomenon via the variations of solvent, anion and substituent.